

# Fractional Fourier Transform Phase for Image Matching

Mariia Protsenko<sup>1</sup> and Elena Pavelyeva<sup>1</sup>

<sup>1</sup> Faculty of Computational Mathematics and Cybernetics, Lomonosov Moscow State University, Leninskie Gory, MSU, Moscow, 119991, Russia

## Abstract

Fractional Fourier transform is the generalization of the Fourier transform. In this article the synthesis of phase and magnitude of fractional Fourier transform is demonstrated. The influence of phase and magnitude on the synthesis results is shown. The fractional phase correlation function using fractional Fourier transform is calculated, and it is used for image matching. The use of fractional phase correlation can achieve better results compared to the use of the classical phase correlation. The comparison between phase correlation and fractional phase correlation for biometric iris images is given. The selection of optimal parameter for fractional phase correlation is proposed.

## Keywords

Fourier transform, Fractional Fourier transform, phase, phase correlation, biometrics, iris recognition.

## 1. Introduction

The Fractional Fourier Transform (FRFT) [1] is the generalization of the classical Fourier Transform. FRFT is used in various signal processing problems [2], [3], [4]. Fractional Fourier Transform is more flexible than classical Fourier Transform since it can be interpreted as a rotation of a signal in the time-frequency plane for a given angle. The FRFT can be used to define fractional convolution [5], fractional correlation, fractional phase correlation [6] and other operations.

The fractional phase correlation function is a generalization of the phase correlation function [7], and both functions can determine the measure of image similarity. The phase correlation method can be used in the various problems of image processing like image registration [8], image mosaicking [9], biometrics [10], [11], motion estimation [12], [13], etc. If two images are similar to each other, then the phase correlation function has a strong peak. The peak value determines the image similarity measure, and its position determines the image shift value.

Biometric identification is widely used nowadays [14]. A person can be identified by the face, fingerprint, iris image, palmprint, finger or palm vein image, ear, etc. Iris recognition is one of the most popular and promising biometric characteristics and can be used in mobile devices [15]. There are a lot of different methods for iris image analysis based on convolutional neural networks or classical mathematical methods, and some iris image analysis methods use the phase information [16], [17], [18].

In this article the iris image matching method based on FRFT phase correlation is presented. This method was tested on iris database CASIA-IrisV4-Interval [19]. The result shows that this approach can be promising to use for human biometric identification.

In the article the FRFT, its phase and magnitude are introduced in Section 2. The synthesis of phase and magnitude of fractional Fourier transform is demonstrated in Section 3. The phase correlation and fractional phase correlation methods are given in Sections 4 and 5. The comparison of phase correlation and fractional phase correlation methods for biometric iris image matching is proposed in Section 6. Section 7 concludes the article.

---

GraphiCon 2022: 32nd International Conference on Computer Graphics and Vision, September 19-22, 2022, Ryazan State Radio Engineering University named after V.F. Utkin, Ryazan, Russia

EMAIL: ma.protsenko@mail.ru (M. Protsenko); pavelyeva@cs.msu.ru (E. Pavelyeva)

ORCID: 0000-0001-5029-4973 (M. Protsenko); 0000-0002-3249-2156 (E. Pavelyeva)



© 2022 Copyright for this paper by its authors.  
Use permitted under Creative Commons License Attribution 4.0 International (CC BY 4.0).

## 2. Fractional Fourier Transform

The Fractional Fourier Transform provides a family of linear transforms for each value of  $a \in R$ . The FRFT of order  $a$  converts the signal  $s(x)$  to the complex signal  $F(\lambda)$  [20]:

$$F^a[s(x)] = F(\lambda) = \int_{-\infty}^{\infty} s(x)K_a(x, \lambda)dx,$$

$$K_a(x, \lambda) = \begin{cases} \frac{1}{\sqrt{2\pi}}\sqrt{1 - ictg\alpha} \exp\left(\frac{i(x^2 + \lambda^2)}{2}ctg\alpha - \frac{ix\lambda}{\sin\alpha}\right), & \alpha \neq 2\pi n \\ \delta(x - \lambda), & \alpha = 2\pi n \\ \delta(x + \lambda), & \alpha = \pi + 2\pi n \end{cases}$$

where  $\alpha = a\pi/2$ .

It can be seen that  $F^a[s(x)] = F^{a+4}[s(x)]$ ,  $a \in R$ . Let's consider some special cases of the value  $a$ .

1. When  $\alpha = \pi/2$ , then  $a = 1$ , and fractional Fourier transform become classical Fourier transform:

$$F^a[s(x)] = F^1[s(x)] = \frac{1}{\sqrt{2\pi}} \int_{-\infty}^{\infty} s(x) \exp(-i\lambda x) dx.$$

2. When  $\alpha = 0$ , then  $a = 0$ , and  $F^0[s(x)]$  reduces to the identity operator.
3. When  $\alpha = \pi$ , then  $a = 2$ , and  $F^2[s(x)]$  is the reflection operator.
4. When  $\alpha = -\pi/2$ , then  $a = -1$ , and the fractional Fourier transform is the inverse Fourier transform.

Thus, the fractional Fourier transform of order  $a$  can be interpreted as the rotation through the angle  $\alpha = a\pi/2$  in time-frequency plane  $(x, \alpha)$ . The different fractional Fourier transform properties, such as the rules of multiplication, division, integration, differentiation, convolution are described in [20], [21]. The various methods for the discrete fractional Fourier transform calculating are also described there.

The fractional Fourier transform can be generalized to the case of two-dimensional images [22], [23]. For some experiments we use two images Lena and Baboon (Figure 1). Let's consider some examples of applying the FRFT to the Lena image. Figure 2 shows the magnitude and phase of the FRFT for various values of the parameter  $a$ .



**Figure 1:** Lena and Baboon original images

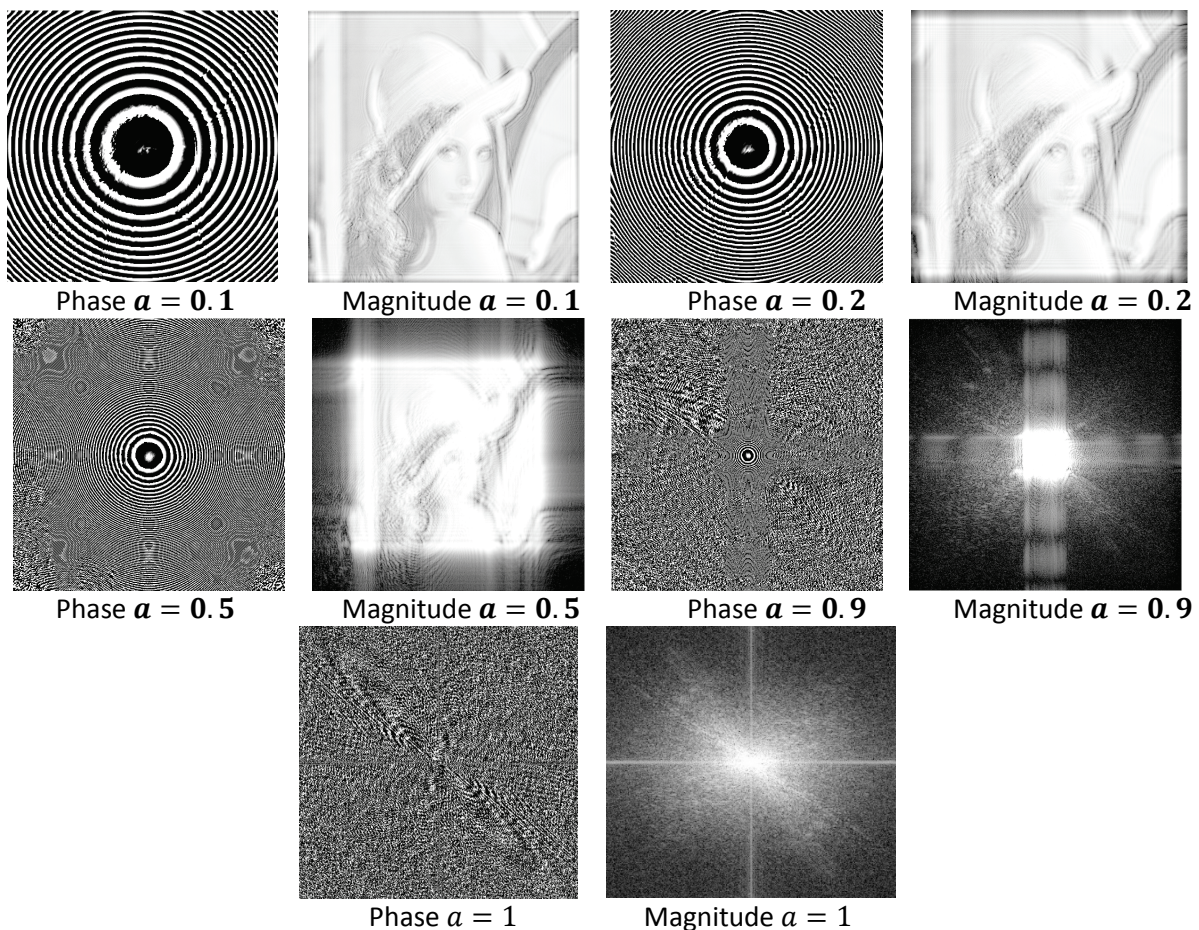


**Figure 2:** Phase and magnitude of the fractional Fourier transform for the Lena image

The FRFT magnitude is presented in a logarithmic scale in all cases. At  $a = 1$  the phase and magnitude of the Fractional Fourier transform are the same as the phase and magnitude of the Fourier transform. When the order  $a$  of FRFT decreases to zero, the FRFT magnitude contains more information about the image structure and image edges than FRFT phase.

### 3. Synthesis of phase and magnitude of fractional Fourier transform

Let's consider the images obtained by synthesis of the FRFT phase of one image and the FRFT magnitude of another image. Two images Lena and Baboon are taken (Figure 1) and their FRFT for different orders  $a$  are calculated.

Let's construct the new synthesis images. We take the FRFT phase of image  $f(x, y)$  and the FRFT magnitude of image  $g(x, y)$ . Then we fix the selected value of  $a$ , calculate fractional Fourier transform for both images  $F(\lambda_x, \lambda_y) = F^a[f(x, y)] = A_f(\lambda_x, \lambda_y)e^{i\varphi_f(\lambda_x, \lambda_y)}$  and  $G(\lambda_x, \lambda_y) = F^a[g(x, y)] = A_g(\lambda_x, \lambda_y)e^{i\varphi_g(\lambda_x, \lambda_y)}$ . After that we combine the FRFT phase  $\varphi_f(\lambda_x, \lambda_y)$  of  $F^a[f(x, y)]$ , and the FRFT magnitude  $A_g(\lambda_x, \lambda_y)$  of  $F^a[g(x, y)]$ , and calculate the FRFT with the order  $-a$ . As a result, we get the new image  $f_1(x, y) = F^{-a}[A_g(\lambda_x, \lambda_y)e^{i\varphi_f(\lambda_x, \lambda_y)}]$ . The results for different values of the parameter  $a$  are shown in Figure 3.

In classical Fourier transform ( $a = 1$ ) the phase contains information about the edges of image. For the fractional Fourier transform, a different amount of information about the edges can contain both the phase and the magnitude, depending on the value of the parameter  $a$ . If  $|a|$  is close to 1, then the phase of the FRFT phase contains more information about the image than the FRFT magnitude. When  $a$  is close to 0 or 2 the phase contains less information about the image. If  $a = 0$  FRFT is the identity

operator, if  $a = 2$  FRFT becomes reflection mapping. In these cases, FRFT phase values are real, not complex. The phase is equal zero and the magnitude contains all information about the given image.

FRFT function is periodical. The period is equal 4.  $F^a[f(x, y)] = F^{a \bmod 4}[f(x, y)]$ .

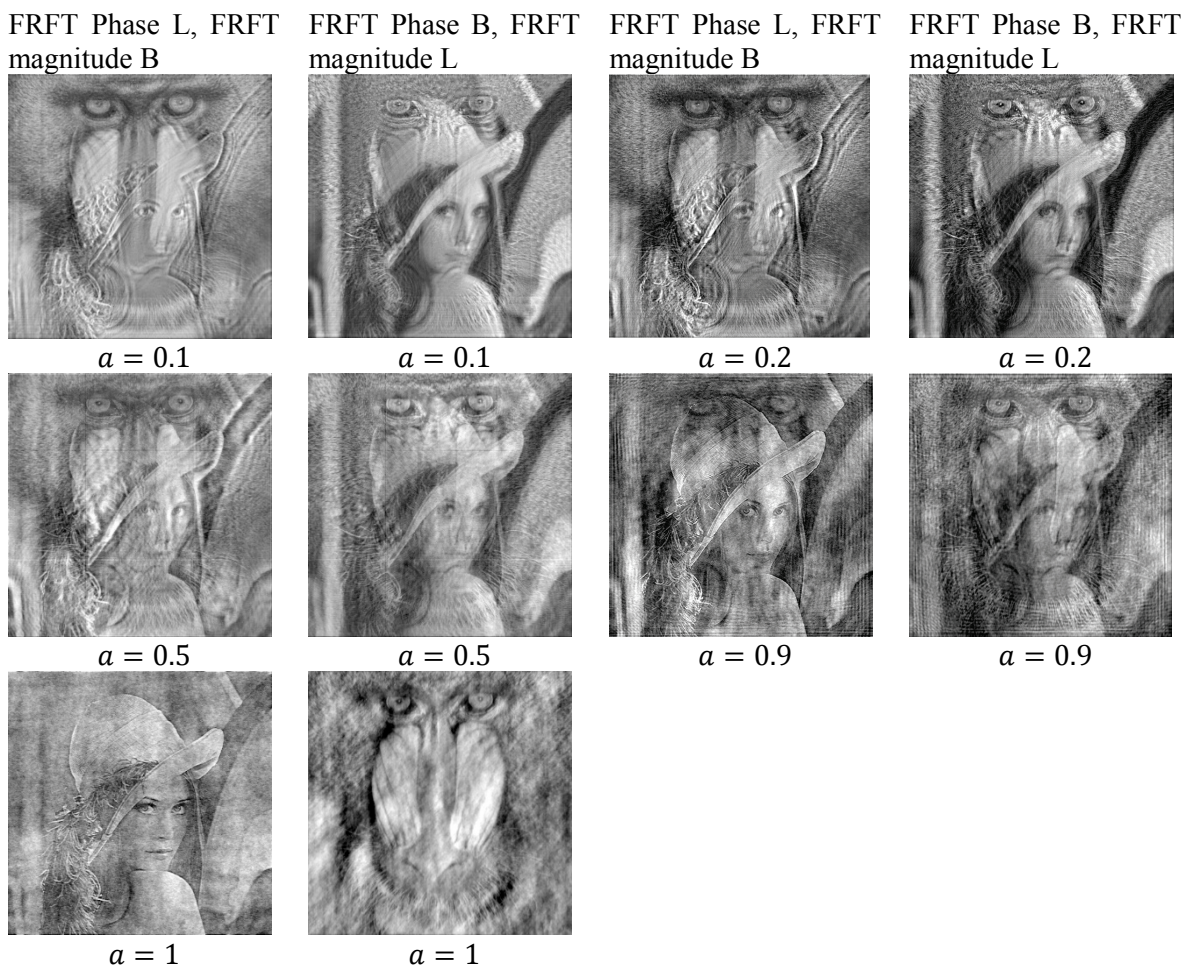


**Figure 3:** Synthesis of the FRFT phase and FRFT magnitude of different images. L – Lena image, B – Baboon image

#### 4. Phase correlation method

Phase correlation method is usually used to find matches between translated, rotated and scaled images [24]. Let  $f(x, y)$  and  $g(x, y)$  are the initial signals. The Fourier transform is a special case of the fractional Fourier transform for  $a = 1$ , and the inverse Fourier transform is the fractional Fourier transform for  $a = -1$ . Therefore  $F(\lambda_x, \lambda_y) = F^1[f(x, y)]$  and  $G(\lambda_x, \lambda_y) = F^1[g(x, y)]$  are the Fourier transforms of the original signals. The cross-phase spectrum is defined as

$$R_{FG}(\lambda_x, \lambda_y) = \frac{F(\lambda_x, \lambda_y) \overline{G(\lambda_x, \lambda_y)}}{|F(\lambda_x, \lambda_y) \overline{G(\lambda_x, \lambda_y)}|} = e^{i(\phi_F(\lambda_x, \lambda_y) - \phi_G(\lambda_x, \lambda_y))},$$

where  $\phi_F(\lambda_x, \lambda_y)$  and  $\phi_G(\lambda_x, \lambda_y)$  are the Fourier transform phases of  $F(\lambda_x, \lambda_y)$  and  $G(\lambda_x, \lambda_y)$ .  $R_{FG}(\lambda_x, \lambda_y)$  is the spectral function with the unit magnitude, and its phase is equal to the difference of the Fourier transforms phases of the original signals. The inverse Fourier transform of  $R_{FG}(\lambda_x, \lambda_y)$  is called as phase-only correlation function (POC-function) or phase correlation function:

$$POC(f, g) = F^{-1}[R_{FG}(\lambda_x, \lambda_y)].$$

If two images are similar to each other, then the phase correlation function has a strong peak. The peak value determines the image similarity measure, and its position determines the image shift value.

Let's consider the example taking Lena image size  $512 \times 512$  pixels and the same image with the cyclic shifts of 40 pixels along the horizontal axis and 30 pixels along the vertical axis (Figure 4). Then we calculate POC-function for a given pair of images (Figure 5).



**Figure 4:** Lena and cyclically shifted Lena

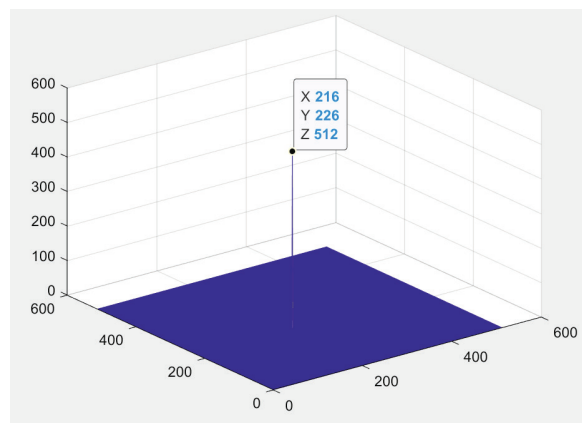


**Figure 5:** POC function values for Lena and cyclically shifted Lena

The resulting graph shows the single strong peak of the POC function. It means that the tested images are similar to each other. The peak is shifted by a vector  $(40,30)$  from the center, that means the displacement  $(40,30)$  between the tested images.

Let's consider the alternative approach to calculating the phase correlation function. We also take two original functions  $f(x, y)$  и  $g(x, y)$ . Next, we introduce a new function  $g_1(x, y) = g(-x, -y)$ . Then we calculate the Fourier transforms for the functions  $g_1(x, y)$  and  $f(x, y)$ :  $G_1(\lambda_x, \lambda_y) = F^1[g_1(x, y)]$  and  $F(\lambda_x, \lambda_y) = F^1[f(x, y)]$ . After that we calculate the values of the spectral function  $R_{FG}(\lambda_x, \lambda_y)$  by the formula [6]

$$R_{FG}(\lambda_x, \lambda_y) = \frac{F(\lambda_x, \lambda_y)G_1(\lambda_x, \lambda_y)}{|F(\lambda_x, \lambda_y)G_1(\lambda_x, \lambda_y)|}$$

Then we apply the inverse Fourier transform to  $R_{FG}(\lambda_x, \lambda_y)$  and obtain the POC-function calculated in the alternative way.

## 5. Fractional phase correlation method

The generalization of the phase correlation method for the fractional Fourier transform is described in [6] and is called as the fractional phase correlation method. This method uses the fractional Fourier transform of different orders instead of the classical Fourier transform. We use the analogue of second

method to calculate the fractional phase correlation function. Let  $F(\lambda_x, \lambda_y) = F^a[f(x, y)]$ ,  $G_1(\lambda_x, \lambda_y) = F^{2-a}[g_1(x, y)]$ . Thus the cross-spectral function can be obtained as

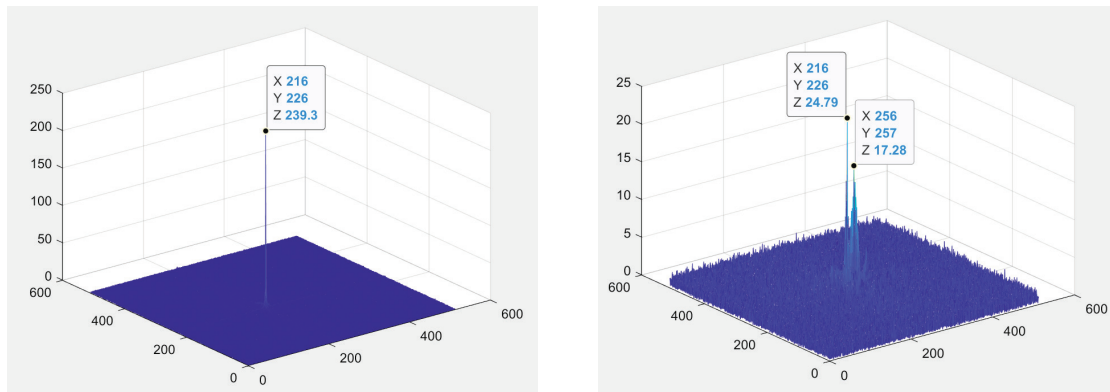
$$R_{FG}(\lambda_x, \lambda_y) = \frac{F(\lambda_x, \lambda_y)G_1(\lambda_x, \lambda_y)}{|F(\lambda_x, \lambda_y)G_1(\lambda_x, \lambda_y)|}$$

Next, we calculate the fractional phase correlation function (fractional POC-function) using the fractional Fourier transform with  $a = -1$ :

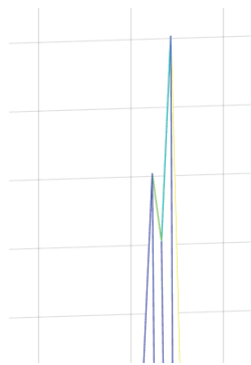
$$POC(f, g) = F^{-1}[R_{FG}(\lambda_x, \lambda_y)].$$

Figure 6 shows examples of fractional POC function for Lena and cyclically shifted Lena. The parameters  $a = 0.99$ ,  $a = 0.97$  were used. The false peak of the fractional phase correlation function appears in the center of the image when the value of the parameter  $|a|$  decreases to zero.

To evaluate the results, we denote the maximum value of the fractional POC-function as  $max_1$  and the second largest local maximum as  $max_2$ . Their ratio is  $v = \frac{max_1}{max_2}$ . The point  $(\lambda_x, \lambda_y)$  will be considered as the point of the local maximum of FRFT if the value of FRFT at this point is greater than the values at all other points  $(i, j), i = \lambda_x - 4, \dots, \lambda_x + 4, j = \lambda_y - 4, \dots, \lambda_y + 4$ . This idea helps us to exclude the situation with multiple peaks (Figure 7).



**Figure 6:** The values of the fractional POC-function at  $a = 0.99$  (left)  $a = 0.97$  (right) for Lena and the cyclically shifted Lena images



**Figure 7:** The example of multiple peaks

## 6. The comparison of phase correlation and fractional phase correlation methods

To evaluate the order  $a$  for calculating the fractional POC-function we use the normalized iris images from the CASIA-IrisV4-Interval database [19]. Figure 8 illustrates the preprocessing of iris images [25]. The algorithm detects iris pupil, eyelashes, eyelids, and then the iris image is normalized into a fixed-size rectangle image, then the contrast enhancement is provided. The example of two normalized iris images of one eye is shown in Figure 9.

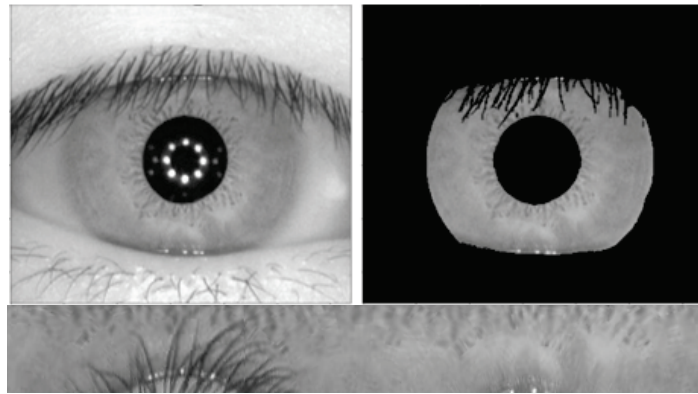


**Figure 8:** Preprocessing of the iris image

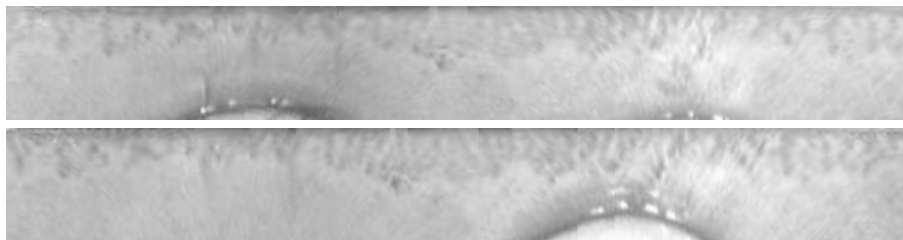


**Figure 9:** Two normalized iris images of one eye

We take a part of the database [19] and compare each iris image with all other iris images. For each compared pair, we use different orders  $a$  for the fractional Fourier transform. Then we calculate the fractional POC function, find the values of  $max_1$  and  $max_2$  and get their ratio  $v = \frac{max_1}{max_2}$ . Next, for each value of the parameter  $a$ , we calculate the average value  $v_{mean}$ . In Figure 10 the dependence between the average values  $v_{mean}(a)$  and the values of the parameter  $a$  is demonstrated. The green solid line shows the dependence for intraclass comparisons, while the red dotted line shows it for the interclass comparisons.

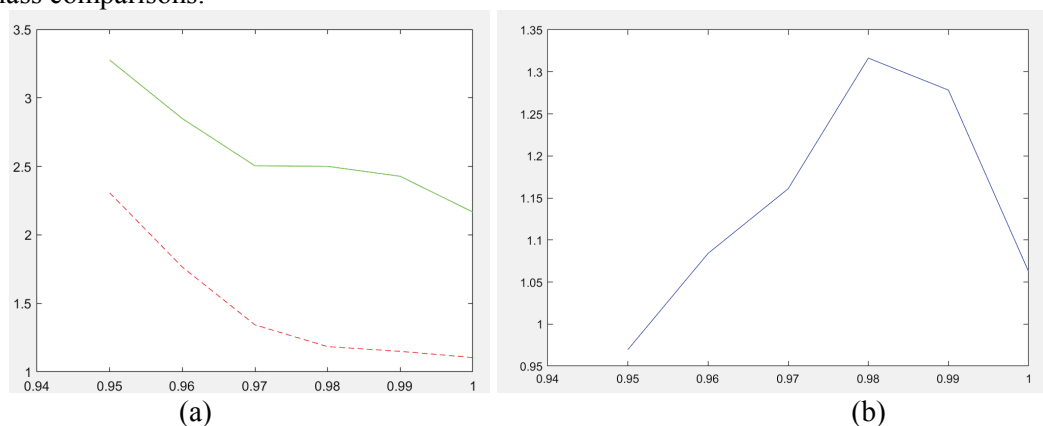


**Figure 10:** (a) Distribution of mean values  $v_{mean}$ . The abscissa shows the values of the order  $a$  of the fractional Fourier transform. The ordinates are  $v_{mean}$ . Green solid line - intraclass comparison, red dotted line - interclass comparison; (b) The difference between the green and red lines

The ratio  $v = \frac{max_1}{max_2}$  is more for images of one eye than for different eye images. The values for  $a = 0.98$  and  $a = 0.99$  are better than for  $a = 1$ . The value  $a = 1$  corresponds to phase correlation method, so the use of fractional POC function allows us to obtain better results than the use of POC function. The best difference between  $v_{mean}(a)$  for pairs of images for one eye and  $v_{mean}(a)$  for pairs of images for different eyes is achieved for  $a = 0.98$  (Figure 10 b). The graph in Figure 10 b shows

that the difference between the average values  $v_{mean}(a)$  for  $a = 1$  is less than  $v_{mean}(a)$  for  $a = 0.97$ ;  $a = 0.98$ ;  $a = 0.99$ . For example, for normalized iris images from Figure 9 the values  $v_{mean}(a)$  for some  $a$  are presented in Table 1.

**Table 1**

Dependence of  $v$  on  $a$  for images from Figure 9

$a$	$v$
1	1.4245
0.99	1.6554
0.98	1.1270

The fractional POC functions for the taken images are presented in Figure 11. However if we take the order  $a = 0.97$  we will have the wrong peak that does not correspond to the shift between images.

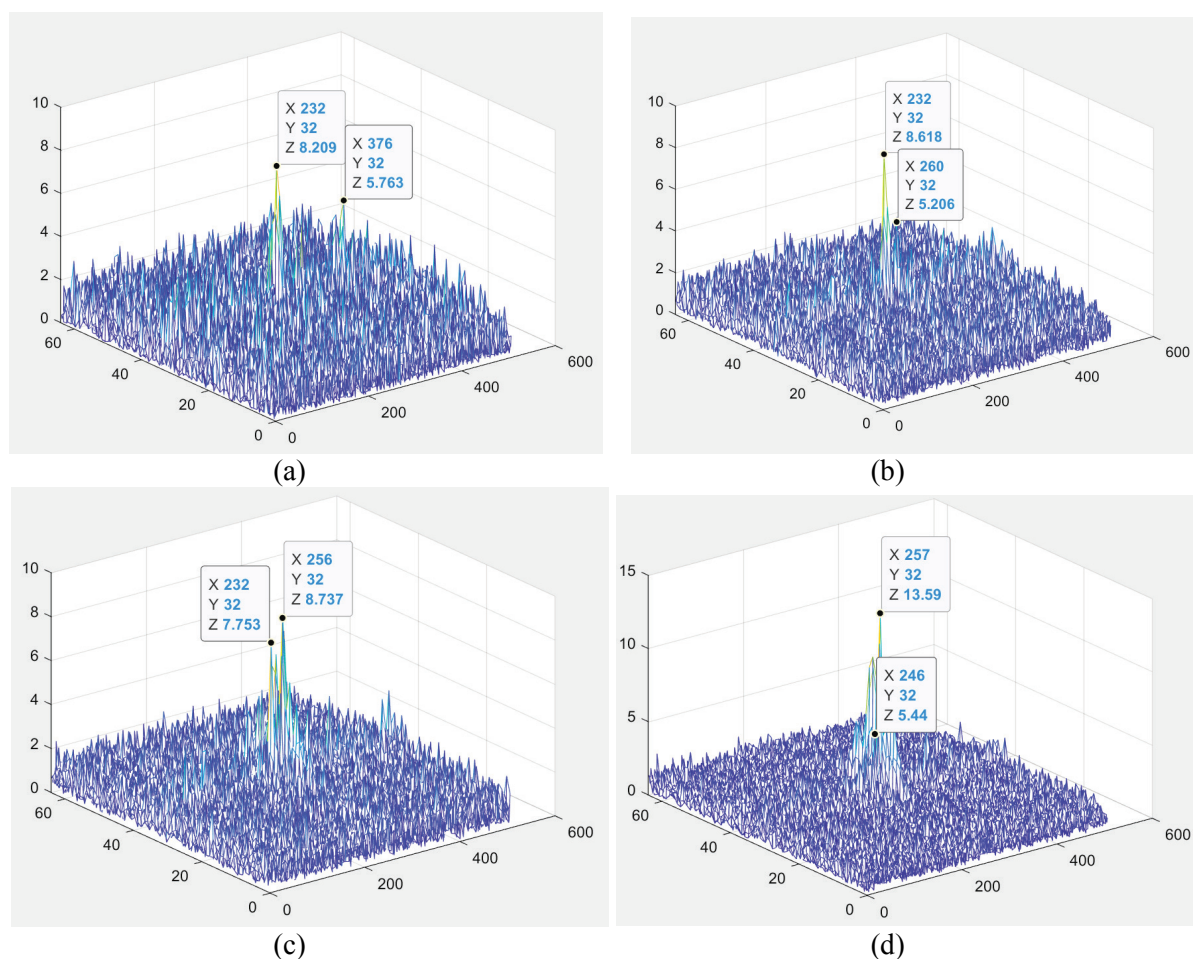


**Figure 11:** Fractional POC functions for different parameter values  $a$  for images from Fig. 9: (a)  $a=1$  (b)  $a=0.99$  (c)  $a=0.98$  (d)  $a=0.97$

As the result, we can conclude that the values of the fractional POC function can be more informative using the orders  $a = 0.99$ ,  $a = 0.98$ . With these values of  $a$ , the fractional Fourier transform phase still contains a significant information about the image's edges, but the noisy information about high frequencies is no longer available. This allows us to blur images and improve the quality of image matching using the fractional POC function.

## 7. Conclusion

In the article the synthesis of FRFT phase and FRFT magnitude for different images is presented. The fractional phase correlation is compared to the phase correlation for normalized iris images matching. The selection of optimal parameter for fractional POC function is proposed. The results show that the use of fractional POC function can be promising in image analysis and biometrics.

## 8. References

- [1] Namias V. The fractional order Fourier transform and its application to quantum mechanics. *IMA Journal of Applied Mathematics*. 1980. V. 25. №. 3. pp. 241-265.
- [2] Erden M. F., Kutay M. A., Ozaktas H. M. Repeated filtering in consecutive fractional Fourier domains and its application to signal restoration. *IEEE Transactions on Signal Processing*. 1999. V. 47. №. 5. pp. 1458-1462.
- [3] Akay O., Boudreaux-Bartels G. F. Fractional convolution and correlation via operator methods and an application to detection of linear FM signals. *IEEE Transactions on signal processing*. 2001. V. 49. №. 5. pp. 979-993.
- [4] Yetik I. S., Nehorai A. Beamforming using the fractional Fourier transform. *IEEE Transactions on Signal Processing*. 2003. V. 51. №. 6. pp. 1663-1668.
- [5] Mustard D. Fractional convolution. *The ANZIAM Journal*. 1998. V. 40. №. 2. pp. 257-265.
- [6] Mendlovic D., Ozaktas H. M., Lohmann A. W. Fractional correlation. *Applied Optics*. 1995. V. 34. №. 2. pp. 303-309.
- [7] Reddy B. S., Chatterji B. N. An FFT-based technique for translation, rotation, and scale-invariant image registration. *IEEE transactions on image processing*. 1996. V. 5. №. 8. pp. 1266-1271.
- [8] Foroosh H., Zerubia J. B., Berthod M. Extension of phase correlation to subpixel registration. *IEEE transactions on image processing*. 2002. V. 11. №. 3. pp. 188-200.
- [9] Jing X. et al. Medical image mosaic technology based on image phase correlation. 2012 Fourth International Conference on Digital Home. IEEE, 2012. pp. 274-277.
- [10] Javed M. Y. et al. Face Recognition Using Processed Histogram and Phase-only Correlation (POC). 2007 International Conference on Emerging Technologies. IEEE, 2007. pp. 238-242.
- [11] Mahri N., Suandi S. A. S., Rosdi B. A. Finger vein recognition algorithm using phase only correlation. 2010 International Workshop on Emerging Techniques and Challenges for Hand-Based Biometrics. IEEE, 2010. pp. 1-6.
- [12] Alexiadis D. S., Sergiadis G. D. Motion estimation, segmentation and separation, using hypercomplex phase correlation, clustering techniques and graph-based optimization. *Computer Vision and Image Understanding*. 2009. V. 113. №. 2. pp. 212-234.
- [13] Namba H., Muneyasu M. A detection and tracking method based on POC for oncoming cars. 2008 International Symposium on Intelligent Signal Processing and Communications Systems. IEEE, 2009. pp. 1-4.
- [14] Kaur N. et al. A study of biometric identification and verification system. 2021 International Conference on Advance Computing and Innovative Technologies in Engineering (ICACITE). IEEE, 2021. pp. 60-64.
- [15] Fartukov A. M., Odinokikh G. A., Gnatyuk V. S. Approaches and Methods to Iris Recognition for Mobile. *Smart Algorithms for Multimedia and Imaging*. Springer, Cham, 2021. pp. 397-422.
- [16] Daugman J. How iris recognition works. *The essential guide to image processing*. Academic Press, 2009. pp. 715-739.
- [17] Pavelyeva E. Image processing and analysis based on the use of phase information. *Computer Optics*. 2018. V. 42. №. 6. pp. 1022-1034.
- [18] Protsenko M. A., Pavelyeva E. A. Image Key Point Matching by Phase Congruency. *Computational Mathematics and Modeling*. 2021. V. 32. №. 3. pp. 297-304.
- [19] CASIA Iris Image Database Version 4.0 URL: <http://biometrics.idealtest.org/dbDetailForUser.do?id=4>.
- [20] Saxena R., Singh K. Fractional Fourier transform: A novel tool for signal processing. *Journal of the Indian Institute of Science*. 2005. V. 85. №. 1. pp. 11-26.

- [21] Tao R., Deng B., Wang Y. Research progress of the fractional Fourier transform in signal processing. *Science in China Series F*. 2006. V. 49. №. 1. pp. 1-25.
- [22] Zayed A. Two-dimensional fractional Fourier transform and some of its properties. *Integral Transforms and Special Functions*. 2018. V. 29. №. 7. pp. 553-570.
- [23] Pei S. C., Yeh M. H. Two dimensional discrete fractional Fourier transform. *Signal Processing*. 1998. V. 67. №. 1. pp. 99-108.
- [24] Reddy B. S., Chatterji B. N. An FFT-based technique for translation, rotation, and scale-invariant image registration. *IEEE transactions on image processing*. 1996. V. 5. №. 8. pp. 1266-1271.
- [25] Tikhonova V. A., Pavelyeva E. A. Hybrid iris segmentation method based on CNN and principal curvatures. *CEUR Workshop Proceedings*. 2020. V. 2744. №. 31. pp. 1-10.